



Regular Articles

Functional analysis of basidiomycete specific chitin synthase genes in the agaricomycete fungus *Pleurotus ostreatus*

Kim Schiphof^a, Moriyuki Kawauchi^{a,*}, Kenya Tsuji^a, Akira Yoshimi^{a,b}, Chihiro Tanaka^{a,b}, Takehito Nakazawa^a, Yoichi Honda^a

^a Graduate School of Agriculture, Kyoto University, Kitashirakawaoiwakecho, Sakyo-ku, Kyoto 606-8502, Japan

^b Graduate School of Global Environmental Studies, Kyoto University, Kitashirakawaoiwakecho, Sakyo-ku, Kyoto 606-8502, Japan



ARTICLE INFO

Keywords:

Chitin
Agaricomycete
Basidiomycete specific chitin synthase
Cell wall
Pleurotus ostreatus

ABSTRACT

Chitin is an essential structural component of fungal cell walls composed of transmembrane proteins called chitin synthases (CHSs), which have a large range of reported effects in ascomycetes; however, are poorly understood in agaricomycetes. In this study, evolutionary and molecular genetic analyses of *chs* genes were conducted using genomic information from nine ascomycete and six basidiomycete species. The results support the existence of seven previously classified *chs* clades and the discovery of three novel basidiomycete-specific clades (BI–BIII). The agaricomycete fungus *Pleurotus ostreatus* was observed to have nine putative *chs* genes, four of which were basidiomycete-specific. Three of these basidiomycete specific genes were disrupted in the *P. ostreatus* 20b strain (*ku80* disruptant) through homologous recombination and transformants were obtained ($\Delta chsb2$, $\Delta chsb3$, and $\Delta chsb4$). Despite numerous transformations $\Delta chsb1$ was unobtainable, suggesting disruption of this gene causes a crucial negative effect in *P. ostreatus*. Disruption of these *chs2–4* genes caused sparser mycelia with rougher surfaces and shorter aerial hyphae. They also caused increased sensitivity to cell wall and membrane stress, thinner cell walls, and overexpression of other chitin and glucan synthases. These genes have distinct roles in the structural formation of aerial hyphae and cell walls, which are important for understanding basidiomycete evolution in filamentous fungi.

1. Introduction

Fungal cell walls play important roles in hyphal morphogenesis, mechanical strength, and interactions with the surrounding environment such as soil, plants, and pathogens (Gow et al., 2017). Generally, in filamentous fungi the major structural components of the cell wall are β -1,3-glucan, chitin, and α -1,3-glucan, to which proteins, and other polysaccharides are bound (Gow et al., 2017). Chitin, a linear polymer of β -(1,4)-*N*-acetyl-D-glucosamine crosslinked via hydrogen bonds to form chitin chains in the cell wall, varies in folding, orientation, and organization (Rogg et al., 2012; Zhou et al., 2019). Once synthesized and elongated, chitin can covalently bond to a side-branch of β -1–3 or β -1–6 glucan to form a glucan-chitin complex which provides the scaffolding for the structure of the cell wall (Bouregghda et al., 2021). Agaricomycete cell walls are assumed to consist of rigid chitin-glucan complexes in the inner cell wall and a more flexible network of β -glucans and other proteins in the outer cell wall (Dalonso et al., 2021). The cell wall

structure of the white-rot agaricomycete *Schizophyllum commune* has previously been analyzed. The inner cell wall is made of different forms of chitin from single stranded to highly branched, as well as β -(1,3), β -(1,3)-(1,6)-glucan, and α -(1,3)-glucan (Ehren et al., 2020). However, the mechanism underlying agaricomycete cell wall synthesis remains poorly understood.

Chitin is vital for cell survival (Brown et al., 2022) and is assumed to be the most ancestral structural polysaccharide in fungal cell walls (Gow et al., 2017). Chitin and its largely deacylated derivative, chitosan, are among the most abundant biological materials after cellulose and have a range of applications, including plant disease resistance, wastewater purification and in biopesticides, agriculture, and medicines (Fernando et al., 2021; Gong et al., 2023). Owing to its range of uses and beneficial properties, chitin is commonly used in industry and has attracted considerable attention as a raw material in the biotechnological, pharmaceutical, and medicinal industries (Choi et al., 2022). Chitin and chitosan from various fungi, including *Pleurotus* and *Lentinula* have been

* Corresponding author.

E-mail address: kawauchi.moriyuki.8c@kyoto-u.ac.jp (M. Kawauchi).

<https://doi.org/10.1016/j.fgb.2024.103893>

Received 29 January 2024; Received in revised form 10 April 2024; Accepted 17 April 2024

Available online 23 April 2024

1087-1845/© 2024 The Author(s). Published by Elsevier Inc. This is an open access article under the CC BY-NC license (<http://creativecommons.org/licenses/by-nc/4.0/>).

investigated as sustainable chitin sources (Abo Elsoud and El Kady, 2019). Furthermore, white-rot fungi, such as *Pleurotus ostreatus* have gained attention as biocatalysts due to their unique ability to degrade all major plant cell wall components, including lignin, which is difficult to hydrolyze and utilize, which implies that they can utilize agricultural waste and woody lignocellulose biomass as sustainable substrates (Haneef et al., 2017). Owing to this unique degradation ability, these fungi can utilize lignocellulose biomass such as wood and agricultural waste as substrate, making the cultivation of white-rot fungi sustainable.

Generally, cell wall chitin is synthesized by a range of chitin synthases (CHSs) and is destroyed or regulated by chitinases in ascomycetes (Gow et al., 2017). CHSs are transmembrane proteins that belong to the glycosyltransferase family 2 (GT2) of processive polymerizing glycosyltransferases (Gonçalves et al., 2016) and have at least one conserved domain (PF03142 or PF01644) and a sequence that corresponds to the QXXRW peptide; however, they can differ widely in their N- and C-termini (Li et al., 2016; Soria et al., 2021). CHSs use UDP-*N*-acetylglucosamine from the cytoplasm to catalyze the formation of *N*-acetyl-D-glucosamine, transport the polysaccharide product out through the membrane, and are assumed to be the limiting enzymes in the cell wall biosynthetic pathway (Chen et al., 2023; Gonçalves et al., 2016; Soria et al., 2021). The knowledge regarding the physiological role of CHSs in basidiomycetes, is limited. In the pathogenic yeast-like basidiomycete *Ustilago maydis*, the loss of *chs5* and *chs7* affects cell shape and hyphal growth, whereas *chs6* and *chs1* are involved in virulence and infection (Weber et al., 2006). In the basidiomycetous yeast *Cryptococcus neoformans*, *chs3* is important for dampening host inflammatory responses, cell growth, and chitosan production (Banks et al., 2005; Hole et al., 2020). In the agaricomycete *Coprinopsis cinerea*, chitin is assumed to be important for fruiting body formation as stipe cell wall extension is associated with the release of *N*-acetylglucosamine (chitin monomer), chitinbiose, and chitinase activity (Zhou et al., 2019), suggesting that CHSs may be required for fruiting body formation or growth. Functional analysis of CHS is limited, except in ascomycetes and basidiomycetous yeasts and the physiological functions of CHSs in white-rot agaricomycetes are unknown. Despite the lack of functional analyses, bioinformatic and enzymatic studies have been conducted. Five putative CHSs in the biotrophic rust fungus *Puccinia graminis* (Broeker et al., 2006), eight putative CHSs in *Ganoderma lucidum* (Wang et al., 2018), one putative CHS in *Agaricus bisporus* (Sreenivasaprasad et al., 2000), and multiple putative CHSs across various studies of the white-rot agaricomycetes *Lentinula edodes* (Nishihara et al., 2007a; Sato et al., 2010) and *P. ostreatus* (Nishihara et al., 2007b) have been previously identified.

In this study, we discovered three novel clades of basidiomycete specific chitin synthase genes and for the first time, physiological function was analyzed in three *chs* genes (*chs2*, *chs3*, and *chs4*) in an agaricomycete. This study aims to improve our understanding of basidiomycete cell wall structure and chitin biosynthesis in agaricomycetes through investigation of *chs* genes.

2. Materials and methods

2.1. Strains, culture conditions, and genetic techniques

The *P. ostreatus* strains used in this study are listed in Table S1. Yeast extract/malt extract/glucose (YMG) medium (Rao and Niederpruem, 1969) solidified with 2 % (w/v) agar in 90 mm Petri dishes was used for routine cultures. Cultures were maintained at 28 °C in continuous darkness. Disruption strains (Δ *chs2*, Δ *chs3*, and Δ *chs4*) were generated through gene targeting with homologous recombination using the 20b strain as a host (Salame et al., 2012). Transformation of *P. ostreatus* was performed using protoplasts prepared from mycelial cells as described previously (Nakazawa et al., 2016; Salame et al., 2012).

2.2. Construction of gene disruption cassettes

Three designed DNA fragments, the upstream and downstream regions of the target gene, and the hygromycin B resistance gene (*hph*) were fused using fusion polymerase chain reaction (PCR). Genomic DNA of *P. ostreatus* PC9 was used as a template to amplify about 1.5 kb of the 5' and 3' flanking regions of *chs1*, *chs2*, *chs3*, and *chs4* with respective primers (Fig. S1, Table S2). The *hph* resistance marker was amplified using the pPHT1 plasmid (Cummings et al., 1999). Each fragment was amplified using Prime STAR GXL polymerase (TaKaRa bio, Shiga, Japan) and fused in the second round of PCR. Fusion primer schematics are shown in Fig. S1. The amplified fragments were purified using a Nucleospin PCR Clean-up and Gel Extraction Kit (TaKaRa bio, Shiga, Japan) and used as disruption cassettes. Details of each disruption cassette are shown in Fig. S1. The primers used for each PCR are listed in Table S2.

2.3. Rapid PCR

Crude genomic DNA from candidate transformants was used as a template (Izumitsu et al., 2012) and PCR was performed using KOD FX Neo DNA polymerase (TOYOBO, Osaka, Japan). The integration of the disruption cassettes was confirmed by PCR amplification of the target gene locus (Fig. S2, S3). To confirm gene disruption, a second PCR was performed using different primer sets. The change in gene length was first examined (Fig. S3A, C, and E), and the presence or absence of the gene was confirmed again (Fig. S3B, D, F). The primers used for the PCRs are listed in Table S2. The details of each primer position and expected length are shown in Fig. S2 and PCR gel electrophoresis results for the corresponding PCRs are shown in Fig. S3.

2.4. Phylogenetic and domain structure analysis

Phylogenetic analysis was conducted using eight known chitin synthases of *Aspergillus fumigatus* (Rogg et al., 2012). Gene homologue searches were conducted using the predicted amino acid sequences for each of the eight reference genes using the Protein-Protein Basic Local Alignment Search Tool (BLASTP) from the National Center for Biotechnology Information (NCBI) (Altschul et al., 1990), Fungi DB (Basenko et al., 2018) and Joint Genome Institute (JGI) (Nordberg et al., 2014) databases. All hits with scores below $1.0 \times E^{-10}$ were selected as putative homologues in *Botrytis cinerea*, *Cochliobolus heterostrophus*, *Coprinopsis cinerea*, *Cordyceps militaris*, *Cryptococcus neoformans*, *Lentinula edodes*, *Morchella importuna*, *Neurospora crassa*, *Pleurotus ostreatus*, *Saccharomyces cerevisiae*, *Schizophyllum commune*, *Schizosaccharomyces pombe*, *Trichoderma reesei*, and *Ustilago maydis*. Phylogenetic analysis was conducted using MEGA11 using the Maximum likelihood method with JTT matrix-based model (Tamura et al., 2021). Further information on the databases used for each strain, corresponding strain names, and protein ID's can be found in Table S3.

The domain architecture was analyzed using the predicted amino acid sequences of CHSs in *P. ostreatus* PC9 obtained from the JGI (Nordberg et al., 2014) (Table S3). The domain architecture was predicted by combining the results of DeepTMHMM (Hallgren et al., 2022) and InterProScan (Jones et al., 2014).

2.5. Southern blot analysis

About 3 μ g of genomic DNA was extracted from each disruption strain and the wild-type using the cetyltrimethylammonium bromide (CTAB) method, as described previously (Muraguchi et al., 2003; Zolan and Pukkila, 1986). Genomic DNA was digested using restriction enzymes followed by size fractionation in 1 % agarose gel and transferred to a positively charged Hybond-N + membrane (Cytiva, Marlborough, MA). Probe labelling, hybridization and detection were conducted using an Amersham Gene Images AlkPhos Direct Labelling and Detection

System (Cytiva, Marlborough, MA). The membrane was hybridised with a probe overnight at 55 °C after which chemiluminescence was visualized using an Amersham Imager 680 system (Cytiva, Marlborough, MA). Details of Southern blot experiments are shown in Fig. S4, and S5.

2.6. Growth and morphological observations

A total of 20 ml of autoclaved YMG agar was dispensed into agar plates (Ø90 mm) and a cork borer (Ø9 mm) was used to inoculate a mycelium plug into the center of each plate. After 10 days of static cultivation under dark conditions at 28 °C, mycelial diameter data was retrieved. Images of mycelia at 10 days on YMG agar were captured using the stereomicroscope SMZ25 (Nikon, Japan) to observe hyphal sparsity.

For aerial hyphae observations, 15 ml of YMG agar was dispensed into test tubes (Ø16 mm) and autoclaved. A cork borer (Ø9 mm) was used to inoculate a mycelium plug into the center of each tube. After 10 days of static cultivation in the dark at 28 °C, images were captured to examine the height of the aerial mycelia at the medium-gas interface.

For transmission electron microscopy (TEM) and scanning electron microscopy (SEM), the 20b strain and all disruptant mutants were cultivated in 20 ml of YMG agar medium at 28 °C for 10 days. Observations were made after fixation and dehydration, as described previously (Han et al., 2023).

For cell wall chitin staining, 40 ml of YMG medium was dispensed into 100 ml flasks and autoclaved. A cork borer (Ø9 mm) was used to inoculate four mycelium plugs into the liquid medium and incubated at 28 °C for 5 days at 120 rpm with shaking. Samples were then homogenized using a polytron homogenizer and 200 µl of the homogenized solution was inoculated into 40 ml of fresh autoclaved YMG liquid medium and incubated at 28 °C, 120 rpm for 2 days. Subsequently, 1 ml of solution was washed with 1 M Tris-HCl and 4 µl 2 % Calcofluor white stain (Sigma Aldrich, St. Louis, USA); in Tris-HCl buffer was added, mixed, and placed on ice for 3 h before fluorescence microscopy was performed on the obtained samples using a confocal microscopy platform STELLARIS (Leica microsystems, Wetzlar Germany).

2.7. Stress and cell wall synthesis inhibitor resistance assay

After autoclaving, YMG agar was supplemented with 5 mM H₂O₂ and 0.02 % sodium dodecyl sulfate (SDS) to test environmental stress resistance; and 100 µg/ml micafungin (MF) and 500 µg/ml calcofluor white (CFW) to test cell wall and oxidative inhibition resistance. Fluorescent Brightener 28 disodium salt solution (Sigma-Aldrich, St. Louis, MO, USA) and Funguard (Astellas, Tokyo, Japan) were used as the CFW and MF, respectively. A control of non-supplemented YMG was also made and a cork borer (Ø9 mm) was used to inoculate a mycelium plug into the center of each plate. After 10 days of static cultivation under dark conditions at 28 °C, images were captured. The colony diameters of the strains on the supplemented plates (D1) and that on YMG were measured (D2). The relative inhibitory rate was calculated as follows: Relative inhibitory rate (%) = (D2 – D1)/D2 * 100.

2.8. Glucan and chitin measurements

For β-glucan and chitin measurements, a total of 20 ml of autoclaved YMG agar was dispensed into agar plates (Ø90 mm). After solidifying, a single layer of autoclaved cellophane was added to cover the entire plate and a cork borer (Ø9 mm) was used to inoculate a mycelium plug into the center of each plate. After 14 d of static cultivation under dark conditions at 28 °C, a sterile spatula was used to harvest aerial hyphae and using a mortar and pestle with liquid nitrogen, mycelia was ground into a powder and freeze-dried.

For α- and β-glucan measurements, a β-Glucan Assay Kit (Yeast and Mushroom) (Megazyme, Ireland) was used to conduct measurements of total glucan in accordance with the total glucan protocol using half

amounts of reagents and samples. Measurements of α-glucan and background glucose were conducted according to manufacturer's protocol using half amounts of reagents and samples. Subsequently, α-glucan amounts were subtracted from total glucan amounts to obtain relative amount of β-glucan in accordance with manufacturer's protocol calculations.

For chitin measurements, 400 µl of 4 N HCl was added to 0.01 g of ground mycelia and heated at 96 °C for 16 h before adding 400 µl of autoclaved water to cool the reaction. Further, ground activated charcoal was added to each sample and vortexed three times over 1 h, after which the sample was centrifuged and 300 µl of supernatant was diluted tenfold using 2.63 ml of autoclaved distilled water and 70 µl of 8 N NaOH to neutralize the sample. The relative percentage of chitin after extraction was determined using a D-Glucosamine Assay Kit (Megazyme, Ireland) in accordance with the manufacturer's protocol.

2.9. Quantitative reverse-transcription PCR (qRT-PCR)

A total of 20 ml of autoclaved YMG agar was dispensed into agar plates (Ø90 mm). After solidifying, a single layer of autoclaved cellophane was added to cover the entire plate and a cork borer (Ø9 mm) was used to inoculate a mycelium plug into the center of each plate. After 14 days of static cultivation under dark conditions at 28 °C, a sterile spatula was used to harvest aerial hyphae and a mortar and pestle with liquid nitrogen was used to grind mycelia into a powder. A FastGene RNA Premium Kit (NIPPON Genetics, Tokyo, Japan) was used to extract RNA. The obtained RNA samples were reverse transcribed using PrimeScript RT Master Mix (TaKaRa bio, Shiga, Japan). PowerTrack SYBR Green Master Mix and QuantStudio 5 (Thermo Fisher Scientific) were used for quantitative PCR. Quantification was performed as previously described (Pfaffl, 2001). All samples and primer pairs were run twice and the mean Ct values were used for calculations. The primer pairs used for the amplification of the cDNA fragments and their amplification efficiencies are listed in Table S4.

3. Results

3.1. Identification of basidiomycete specific CHSs and phylogeny across basidiomycetes and ascomycetes

Fungal CHSs have been predicted bioinformatically and can be classified into seven classes (I–VII) based on amino acid homology with variations in the number of *chs* genes in different species. Classes I, II, and IV are present in all fungi; whereas classes III, V, VI, and VII are specific to filamentous fungi. Individual CHSs are likely to perform specific and distinct functions (Gow et al., 2017; Rogg et al., 2012). CHS classifications were initially based on ascomycete classification systems and have not been suitably adapted to other fungi, such as basidiomycetes. Utilizing 112 deduced amino acid sequences from nine ascomycete and six basidiomycete species, phylogenetic analysis was conducted to investigate the relationship between chitin synthases across phyla (Fig. 1 and Table 1). Seven classes of predominantly ascomycete *chs* genes have been previously identified (Rogg et al., 2012). The results indicated that, seven *chs* gene classes were present and were grouped in divisions (Fig. 1). The phylogenetic analysis indicated the presence of three novel basidiomycete-specific classes (BI, BII, and BIII).

Four candidate basidiomycete-specific chitin synthase (*chsb*) genes were identified in *Pleurotus ostreatus*. ID numbers indicate the protein ID numbers in JGI (Fig. 1). We renamed the *P. ostreatus* chitin synthases in accordance with their most similar homologs in *A. fumigatus* and will hereafter be referred to by the names in Table 1.

Classes BI and BII are unique clades in division I and are not members of classes I, II, or III. BIII is in division II and is the distinct clade most closely related to class IV. The results confirmed class VI as ascomycete-specific, in accordance with previous classifications (Liu et al., 2017). Class BI contained only one CHS protein per species, whereas class BII

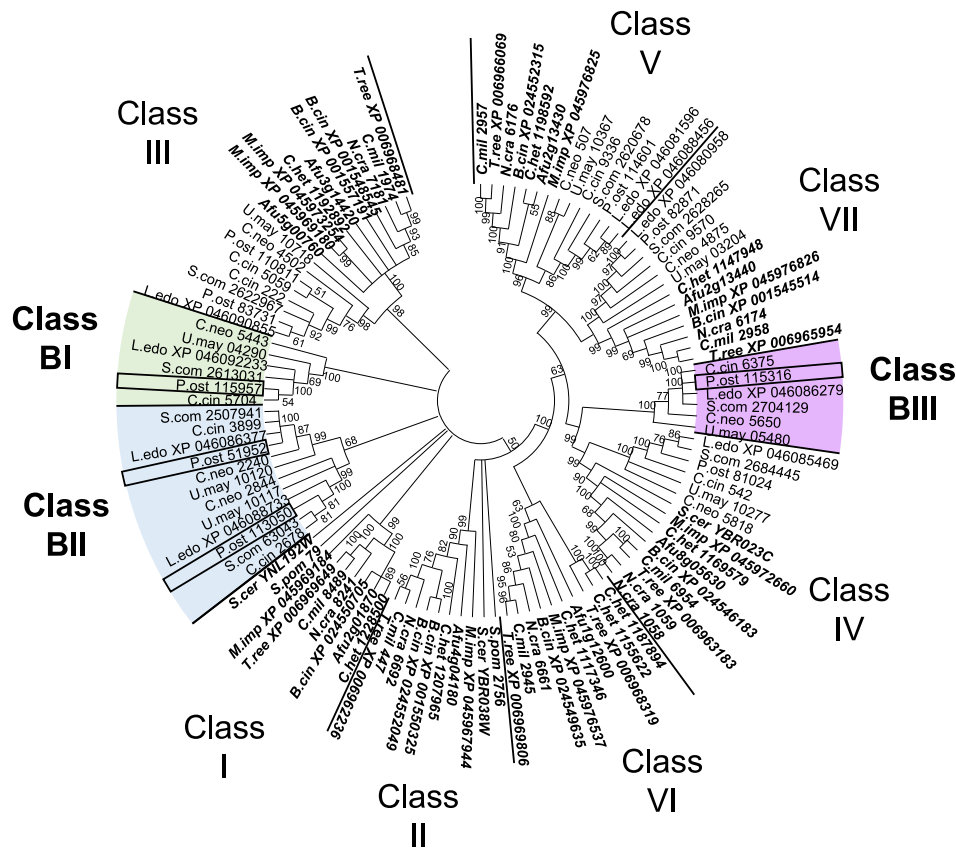


Fig. 1. Phylogeny of predicted *chs* genes. Phylogeny conducted using 112 amino acid sequences. The Maximum Likelihood method and JTT matrix-based model. Bootstrap values inferred from 1000 replicates. Branches corresponding to partitions reproduced in less than 50% bootstrap replicates were collapsed. Numbers above branches represent percentage of replicate trees in which associated taxa clustered together in the bootstrap replicates. Basidiomycetes are indicated by normal text and ascomycetes in bold italics. Accession number, protein ID, database, and species name acronym details are listed in Table S4.

contained duplicates for each species.

Each chitin synthase in *P. ostreatus* contained a conserved domain of either PF03142 or PF01644 (Fig. 2). *Chsb1*, *Chsb2*, *Chsb3*, *Chs7*, and *Chs9* have similar domain architectures, with an N-terminus, a conserved PF01644 region at the N-terminus, and transmembrane domains at the C-terminus. *Chs8* and *Chs5* contain a myosin motor domain (MMD), a characteristic of class V and VII chitin synthases, respectively. *Chsb4* and *Chs6* have slightly different domains, with a PF03142 domain and transmembrane domains at both the N- and C-terminus. According to previous classification requirements (Li et al., 2016; Liu et al., 2017) *chs4* and other clade BIII genes are type B1 genes whilst *chs1–3* and others in clades BII and BI are type A2 genes. Two basidiomycete CHSs (*S.com_2613031* and *U.may_04290*) have unclassified types, as they both contain a glycosyltransferase domain (PF13632) that has not been associated with any previous CHS domain structures or types (Fig. S6 and Table S4). Hydropathy and transmembrane analyses indicated that all genes possessed multiple transmembrane domains (Fig. 2) (Liu et al., 2017; Pacheco-Arjona and Ramirez-Prado, 2014). All basidiomycete-specific CHSs have six transmembrane domains, except for *Chsb2* which has eight transmembrane domains. CHSs have various combinations of domains. All yeasts and filamentous fungi contain three conserved motifs, QXXEY, (E/D)DX, and Q(R/Q)XRW. These conserved regions are observed in a short stretch of the peptide known as Conserved Region 1 (CON1), which also forms the core of the Chitin Synthase 2 domain (CS2: PF03142) (Pacheco-Arjona and Ramirez-Prado, 2014). Putative CON1 regions were observed in all *P. ostreatus* CHSs and were also determined for each basidiomycete-specific CHS of interest and found in the appropriate locations, indicating that these predicted proteins are likely true chitin synthases. Classes IV–VII contain the chitin synthase 2 (CS2: PF03142) domain, whereas classes I–III have

been assumed to have lost the first portion of CS2 and have a chitin synthase domain (CS1: PF01644) and a chitin synthase N-terminal domain (CS1N: PF08407), while still preserving the CON1 found in CS2 (Liu et al., 2017). Additionally, class I has conserved motifs present in the amino-terminal portion; classes IV, V, and VII contain a binding domain similar to cytochrome b5 (CYT-b5: PF00173). Classes V and VII also contain a myosin motor domain (MMD: PF00063) and sometimes a DEK C-terminus (DEKc: PF08766) (Fig. S3) (Li et al., 2016; Pacheco-Arjona and Ramirez-Prado, 2014). Class IV has been speculated as the common ancestor of all fungal *chs* genes (Pacheco-Arjona and Ramirez-Prado, 2014). Smaller subclasses of *chs* have also been identified in class VI (Li et al., 2016).

Division I consists of classes I, II, and III; division II consists of classes IV, V, and VII; and division III consists only class VI (Liu et al., 2017). Within these divisions, division II has been previously suggested to consist of four orthologous clades: V, VII, IVa, and IVb; whereas division III consists of three distinct orthologous clades: Vía, Vīb, and Vīc (Li et al., 2016). Class VI (division 3) has not previously been found in Basidiomycota (Liu et al., 2017). In a previous study, a *chs* in *P. ostreatus* was isolated and classified (Nishihara et al., 2007b). We conducted a reverse BLAST search using this gene, which had 98 % similarity to *P. ost* 81024, which we have renamed to *chs6* because of its similarity to *Aspergillus fumigatus* CHSF (Table 1). Nishihara et al. further classified this gene as a class IV gene and our phylogenetic analysis supports this classification, with *chs6* falling into class IV (Fig. 1) (Nishihara et al., 2007b).

3.2. Disruption of *chs2–4* alters aerial hyphae morphology

The physiological functions of agaricomycete chitin synthases have

Table 1
Chitin synthase genes in *P. ostreatus*.

Gene name	Corresponding <i>chs</i> class	Protein ID ^b
<i>chs1</i>	BI	115,957
<i>chs2</i>	BII	113,050
<i>chs3</i>	BII	51,952
<i>chs4</i>	BIII	115,316
<i>chs5</i>	VII	82,871
<i>chs6</i> ^a	IV	81,024
<i>chs7</i>	III	110,811
<i>chs8</i>	V	114,601
<i>chs9</i>	III	83,731

^a Previously identified and enzymatically analyzed as *Pochs1* (Nishihara et al., 2007b).

^b Protein ID from the genome database of strain PC9 (JGI *Pleurotus ostreatus* PC9 v1.0, https://genome.jgi.doe.gov/PleosPC9_1/PleosPC9_1.home.html).

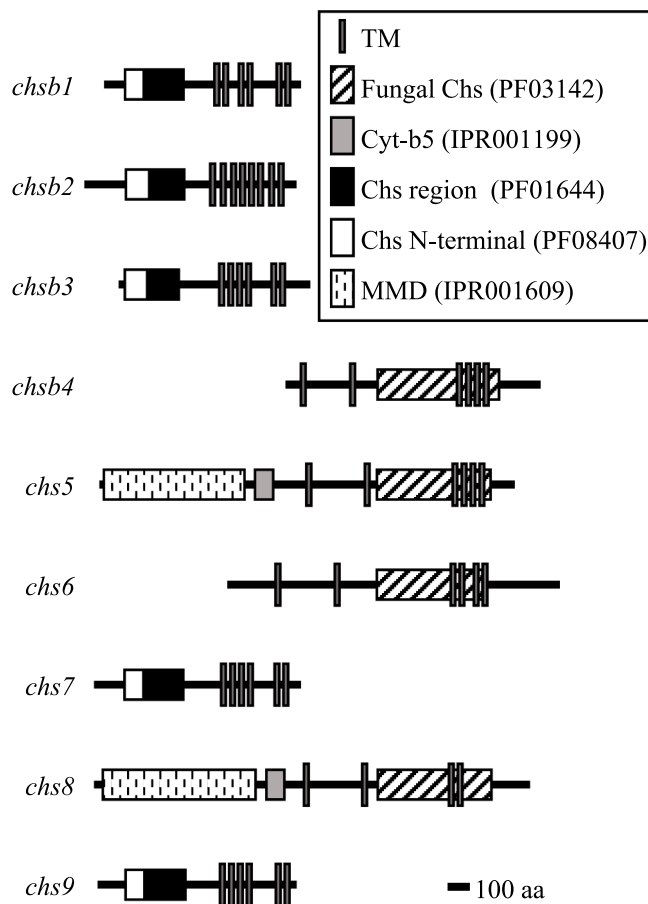


Fig. 2. Domain structures of the nine predicted chitin synthases (CHSs) in *P. ostreatus*. Chs, chitin synthase domain; Cyt-b5, cytochrome b5-like heme/steroid binding domain; MMD, myosin motor domain; and TM, transmembrane domain.

not yet been analyzed. Given the presence of three clades of basidiomycete-specific *chs* genes (Fig. 1), important and specific *chs* roles may be present that could help in understanding agaricomycete evolution and function. To investigate the function of agaricomycete CHS, we disrupted three basidiomycete-specific *chs* genes in *P. ostreatus* and investigated their morphological effects. Disrupted strains were obtained for *chs2–4* (Figs. S3 and S5). Six candidates were obtained for *chs2*, two of which were true disruptants and strains $\Delta chs2\#1$ and $\Delta chs2\#2$ selected for further analyses. Five candidates for *chs3* were obtained, all of which were true disruptants and $\Delta chs3\#1$ and $\Delta chs3\#2$ were selected for further analyses. Four candidates were

obtained for *chs4*, three of which were true disruptants and $\Delta chs4\#1$ and $\Delta chs4\#2$ were used for further experiments (Figs. S3 and S5). *chs1* disruptants were not obtained despite numerous attempts, likely because they play a critical role in growth and were therefore not investigated in this study. Observation and measurement of colony diameter growth on YMG agar plates revealed no apparent differences between any of the disruptants ($\Delta chs2$, $\Delta chs3$, and $\Delta chs4$) and the wild-type 20b strain (Fig. 3A, E). Despite having no impact on growth rate, the mycelia of all three deletion strains were much sparser than those of the wild-type (Fig. 3B). Furthermore, the mycelial surfaces were rougher in all three deletion strains (Fig. 3C). Aerial hyphae on YMG agar cultures were also much shorter in deletion strains than those in the wild-type, especially in $\Delta chs2$ and $\Delta chs3$ strains (Fig. 3D). These results suggest that *chs2–4* are involved in normal vegetative mycelia, especially aerial hyphae, formation in *P. ostreatus*.

3.3. Microscopy indicates *chs2–4* have strong impacts on cell wall thickness and mycelial sparsity

To further understand the impact of basidiomycete CHSs on hyphal formation, we investigated hyphal sparsity, cell wall effects, and chitin localization in all three *chs* deletion strains. Scanning electron microscopy (SEM) further revealed that the hyphae were less sparse, suggesting altered hyphal density (Fig. 4A). Transmission electron microscopy showed that cell walls were drastically thinner in all three deletion strains, especially $\Delta chs2$ and $\Delta chs3$ strains with cell wall thickness dropping from approximately 107 ± 6.3 nm to 53 ± 6.6 nm and 58 ± 5.2 nm, respectively (Fig. 4B). $\Delta chs4$ strains also had significantly thinner cell walls compared to the wild-type strain, however, slightly thicker than the other deletion strains at approximately 82 ± 7.7 nm (Fig. 4B, C). Chitin localization was also investigated, as CHSs have previously been associated with the presence of chitin in both the hyphal septum and tips of various ascomycetes (Ichinomiya et al., 2005; Jin et al., 2021; Rogg et al., 2012; Silverman et al., 1988). However, CFW staining indicated the presence of chitin in the septum and tips of all strains (Fig. 4D). However, $\Delta chs2$ and $\Delta chs3$ strains were more difficult to stain and CFW staining was much fainter and not as clear as the wild-type or $\Delta chs4$ strains, suggesting different contribution to these structures between *chs2,3*, and *chs4*. Hyphal thickness was also investigated and no change was observed (Fig. 4E), suggesting a change in mycelial density in all three disruption strains, which may also be related to the mycelial sparseness observed during stereomicroscopy (Fig. 3B).

3.4. Relative amount of chitin and β -glucan did not change despite differential expression of various cell wall synthases in response to *chs2–4* disruption

Given the difficulty of CFW staining and the significantly decreased cell wall thickness, we investigated whether these effects were due to a change in the relative amounts of chitin and glucan. Relative amounts of chitin (g/100 g dried mycelia) remained almost unchanged in all deletion strains, except for a small increase in relative amount of chitin from 4.1 % in the wild-type to 4.6 % and 5.1 % in $\Delta chs2$ strains (Fig. 5A). Similarly, relative amounts of β -glucan and α -glucan (g/100 g dried mycelia) were also unchanged (Fig. 5B and C). Disruption of *chs2–4* did not alter relative ratio of chitin and β -glucan in the cell wall. Owing to the thinner cell walls (Fig. 4), the contents of chitin and β -glucan per length mycelia may have decreased, although the possibility that configurational changes could have increased the cell wall density in the transformants cannot be ruled out.

Further, we investigated cell wall synthase gene expression levels to determine partial redundancy or other gene relationships. When observing relative gene expression levels across all nine chitin synthases, two β -glucan synthases and single α -glucan synthase in *P. ostreatus*, $\Delta chs2$ and $\Delta chs3$ strains exhibited very similar expression patterns

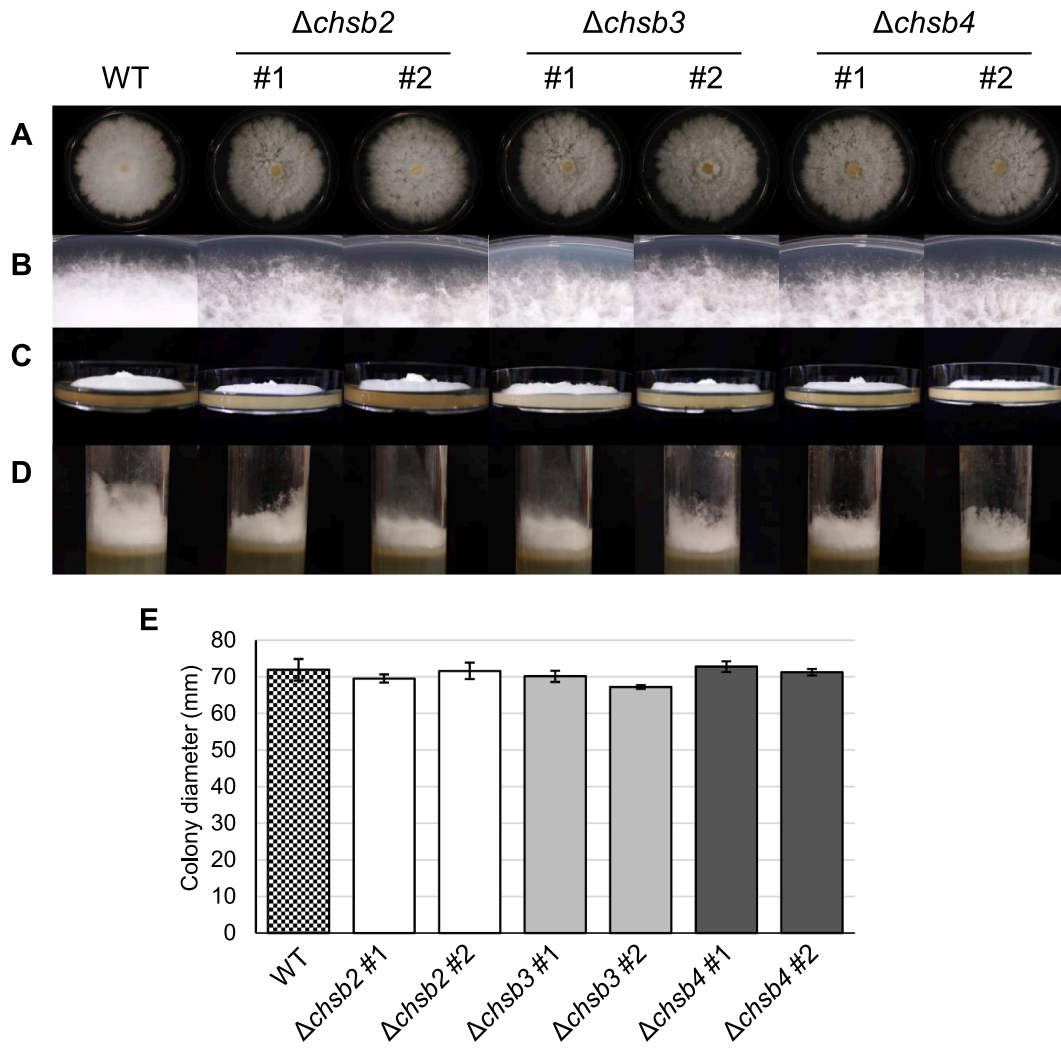


Fig. 3. Morphology, growth rate, and aerial hyphae assay of the wild-type (WT) and transformants. (A–C) Effect of *chs2–4* disruption strains on growth morphology of mycelium grown on yeast and malt extract with glucose (YMG) agar at 10 days with (A) growth morphology, (B) mycelium under stereomicroscopy, and (C) side view of hyphae on plates. (D) Effect of *chs2–4* disruption strains on aerial hyphae formation. (E) Colony diameter of WT and transformants on YMG agar at 10 days. All bars indicate the standard deviations of three biological replicates ($n = 3$). Statistical significance was determined by a two-tailed equal variance *t*-test.

with the highest overexpression being eightfold and tenfold overexpression in *chs4* (Fig. 6). In Δ chs2 and Δ chs3 strains the next highest overexpressed gene was *chs1* followed by *chs7*, *fks1* (β -glucan synthase 1), *ags1* (α -glucan synthase 1), *chs5*, and *chs9* (Fig. 6A and B). Δ chs4 strain exhibited different gene expression patterns with the highest overexpression being a three to fourfold overexpression of *chs7* followed by a twofold overexpression of *fks1* (Fig. 6C). There are clear attempts at compensation by various other cell wall synthase genes and a relationship with various other chitin synthases as well as α and β -glucan synthases can be observed.

3.5. Disruption of *chs2–4* impacts sensitivity to cell wall and cell membrane inhibitors and not oxidative stress

In addition to its importance for growth and morphology, the cell wall plays an important role in protecting cells from external harm and regulating environmental interactions (Ene et al., 2015; Gow et al., 2017). To determine whether basidiomycete-specific CHS function extends beyond a structural role, we investigated whether cell wall integrity and the ability to defend against environmental stress were altered by *chs* deletion. Significantly increased sensitivity to calcofluor white (CFW), a chitin inhibitor; micafungin (MCF), a β -glucan synthesis inhibitor; and sodium dodecyl sulfate (SDS), a membrane degrader was

found in all three deletion strains (Fig. 7). CFW had the largest impact increasing inhibition from about 15 % in the wild-type to over 40 % in Δ chs strains (Fig. 4B). Despite differences in cell wall and cell membrane stressors, no significant differences were observed in sensitivity to H_2O_2 , an oxidative stressor. These results suggest *chs2–4* plays specific roles in cell wall and membrane regulation but not in overall cell oxidation or respiration.

4. Discussion

In this study, we identified novel clades of basidiomycete-specific chitin synthases (*chs*) and for the first time analyzed their physiological functions in agaricomycetes and white-rot fungi. We found three basidiomycete-specific chitin synthase classes, in addition to the existing seven classes as outlined in a previous phylogenetic analysis of model ascomycetes and pathogenic yeasts (Fig. 1) (Rogg et al., 2012). The novel basidiomycete-specific classes are called classes BI–BIII. BI and BIII contained one chitin synthase per species, whereas BII contained duplicates with two chitin synthases per species, suggesting a possible redundancy within this class. Previously, phylogenetic and domain classification of CHSs were based on ascomycete phylogeny; however, since expanding CHS investigations to different phyla, many different subclasses and clades have been identified, which vary across the

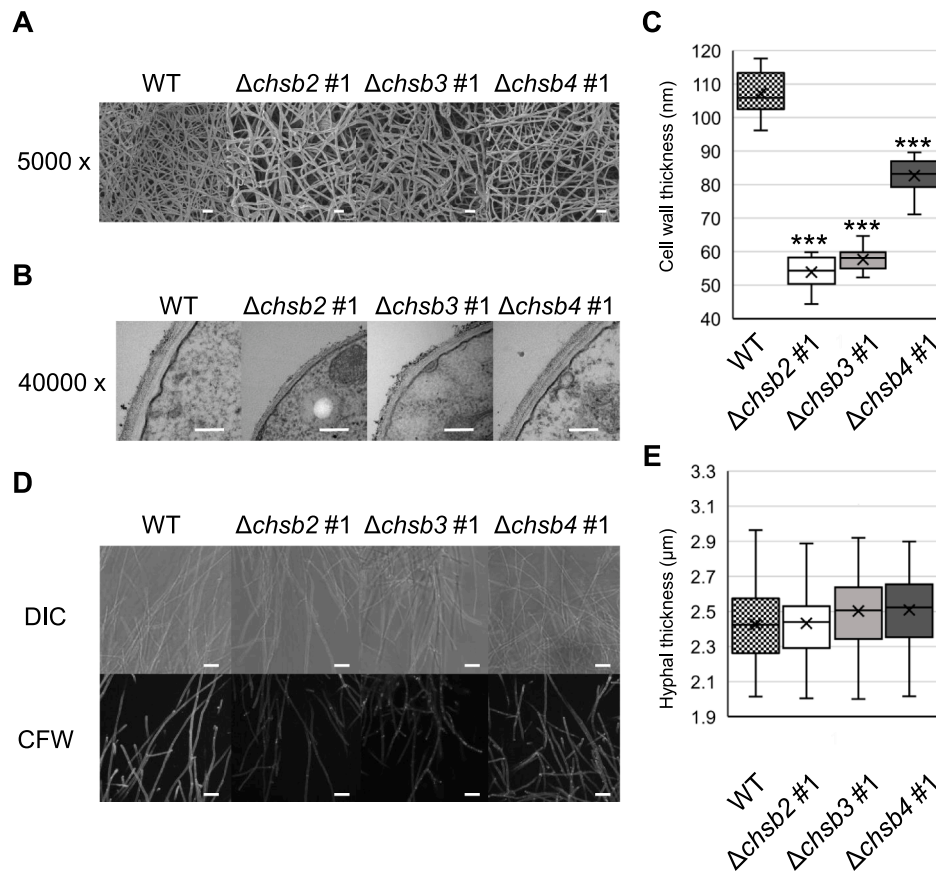


Fig. 4. Impacts of *chs2–4* on cell wall structure and hyphal thickness of mycelia on yeast and malt extract with glucose (YMG) agar at 10 days. (A) Scanning electron microscope (SEM), bar = 10 μm . (B) Cell wall transmission electron microscopy (TEM), bar = 200 nm. (C) Measurements of cell wall thickness under TEM observations, the bars indicate the standard deviations of twenty cell walls of each strain ($n = 20$). Statistical significance was determined using a two-tailed equal variance t -test ($***P < 0.001$). (D) Calcofluor white (CFW) staining for chitin localization, bars = 20 μm . DIC, differential interference contrast. (E) Hyphal width, the bars indicate standard deviation of fifty hyphae of each strain ($n = 50$). Statistical significance was determined using a two-tailed equal variance t -test.

literature owing to the complexity of CHS evolution and their large range of functions across species (Gonçalves et al., 2016; Li et al., 2016; Liu et al., 2017; Pacheco-Arjona and Ramirez-Prado, 2014; Rogg et al., 2012). Domain analysis revealed that all basidiomycete-specific CHSs in *P. ostreatus* contained the domains required for chitin synthases (Fig. 2); however, domain analysis suggested that previous classification systems based on domain architecture are not always accurate and cannot be used to predict the CHS class or division (Table S4). Although previous studies have suggested the existence of basidiomycete subgroups (Gonçalves et al., 2016), our results suggest that basidiomycete clades are distinct classes and not subgroups within existing classes. Furthermore, comparative genomic data have previously revealed an orthogroup of CHSs in agaricomycetes that are significantly upregulated in the primordia stage (Nagy et al., 2023) and chitin is known to be important in agaricomycete fruiting body stipe elongation (Zhou et al., 2019), further suggesting the existence of basidiomycete-specific CHSs and chitin roles. Despite the previous identification of candidate *chs* genes, this study is the first to analyze the physiological functions and roles of agaricomycete CHSs. *Pleurotus ostreatus* has four basidiomycete-specific chitin synthase genes *chs1*, *chs2*, *chs3*, and *chs4* (Table 1). This study was conducted using $\Delta chsb2–4$ strains as *chs1* transformants were difficult to obtain or isolate and therefore likely has some important role in growth and mycelial function.

Disruption of *chs2–4* did not affect the growth rate of the mycelium; however, caused sparser mycelia (Fig. 3), and aerial hyphae were also found to be shorter, suggesting that *chs2–4* plays a role in normal hyphal formation and affects the ability of aerial hyphae to physically support themselves. Similarly, rougher mycelial surfaces highlight a loss

of the ability to form normal mycelial mats. These morphological changes suggest an important relationship between *chs2–4* and normal hyphal and mycelial formations.

Electron microscopy revealed that the cell walls were significantly thinner in all *chs2–4* disruption strains (Fig. 4), suggesting that they play a role in cell wall structure, which likely also contributes to the abnormal mycelial mat formation and growth defects observed in aerial and vegetative hyphae. Although the cell walls were thinner in all disruption strains, $\Delta chsb2$ and $\Delta chsb3$ strains were much thinner than not only the wild-type but also $\Delta chsb4$ strains, suggesting *chs2/chsb3* have similar roles to each other, however, are functionally different to *chs4*.

A previous study in the filamentous ascomycete *Aspergillus nidulans* revealed that class I and class II CHS impacted septum chitin formation (Ichinomiya et al., 2005); however, when we investigated chitin localization through CFW staining and fluorescence microscopy, our results suggested that *chs2–4* are not essential for septum chitin formation, as all disruption strains showed staining at both the septum and tips. However, the *chs2* and *chs3* deletion strains were more difficult to stain and showed fainter results, with seemingly more background or nonspecific CFW binding. The wild-type strain and *chs4* disruptant did not experience this phenomenon and produced clear bright results, further suggesting a functional difference between *chs2/chsb3* and *chs4* (Fig. 4D, E). Further investigation is needed to determine the exact functional differences between these genes. However, because of their different binding capabilities with CFW and changes in cell wall thickness, they may have roles in the amount, distribution, folding structure, or CFW-binding capability of cell wall chitin. Furthermore, phylogenetic

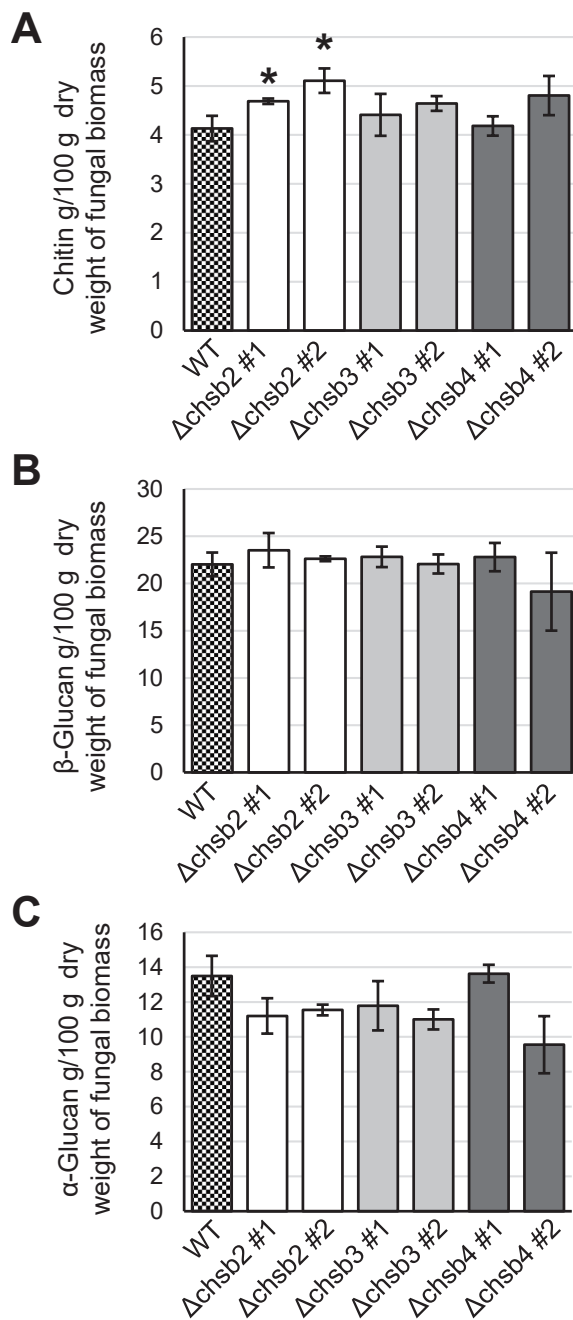


Fig. 5. Percentage of mycelial dry weight made up of (A) chitin, (B) β -glucan, and (C) α -glucan from mycelia on yeast and malt extract with glucose (YMG) cellophane at 14 days old. The bars indicate the standard deviations of three biological replicates ($n = 3$). Statistical significance was determined using a two-tailed equal variance t -test ($*P < 0.05$).

analysis placed both *chs2* and *chs3* in clade BII, whereas *chs4* was placed in clade BIII, suggesting that the functional differences between basidiomycete-specific genes are related to their phylogenetic classes. However, despite *chs2* and *chs3* being in the same class, they were not completely redundant with each other, as morphological, cell wall, and CFW staining impacts were still observed in all single deletion strains for both genes. This highlights an interesting evolutionary pattern in which two genes in the same clade have seemingly identical functions and effects that are not completely redundant. The total amount of *chs2* and *chs3* expression may be important for maintaining normal cell wall structure in this fungus.

Chitin and glucan assays showed that disruption of *chs2–4* does not alter the relative percentage of β -glucan content per weight mycelia (g/100 g) and only has a slight impact in relative chitin percentage (g/100 g) in Δ *chs2* strains (Fig. 5). Given that the cell wall is the predominant factor in mycelial dry weight, the distribution or amount of chitin per unit length of mycelia might have reduced, as the cell walls were significantly thinner in all disrupted strains (Fig. 4B). β -glucan usually binds to chitin to anchor it to the membrane and α -glucan binds to β -glucan (Bouregghda et al., 2021); therefore, if the amount of chitin per length of mycelium is decreased the amount of β -glucan and subsequently α -glucan per length of mycelium will also decrease as there is nowhere to bind to and this likely causes the thinner cell wall phenotype observed. In contrast, chitin has multiple configurations, folding patterns, and structures ranging from linear to highly branched (Fernando et al., 2021; Rogg et al., 2012); therefore, conformational changes might have occurred that increased the density of the cell wall and altered the cell wall thickness in this fungus.

Relative gene expression level analysis of *chs2–4* disruption strains highlighted that deletion of *chs* leads to overexpression, though not underexpression of many other cell wall synthase genes including β -glucan (*fks*) and α -glucan (*ags*) synthases (Fig. 6). Again, *chs2* and *chs3* disruption strains showed similar results and differed from *chs4* disruption strains, further supporting the existence of functional differences between these genes. In *chs2* and *chs3* disruption strains the highest overexpression was observed in *chs4*, *chs1*, *chs7*, *fks1*, and *ags1*. In *chs4* disruption strains the highest overexpression was observed in *chs7* and *fks1*. Despite Δ *chs2* and Δ *chs3* strains causing over an eightfold overexpression in *chs4* this relationship was not reciprocated as Δ *chs4* strains did not cause a large overexpression in *chs2* or *chs3*. Furthermore, the expression level of *chs7*, the highest overexpressed gene in Δ *chs4* strains, only increased fourfold; whereas in Δ *chs2* and Δ *chs3* strains, the highest overexpressed gene *chs4* was expressed upwards of eightfold higher, further supporting these genes as being functionally different. Gene disruption of *chs2–4* also caused significantly thinner cell walls, suggesting a decrease in chitin per unit length of mycelia despite the overexpression of many cell wall synthases, including chitin synthases. This suggests that no true compensatory mechanism has evolved in *chs2–4* genes; despite the overexpression of many genes to make up for gene disruption, strong vegetative mycelia and cell wall impacts are still observed.

In ascomycetes, CHSs are also known to have impacts on virulence, stress response, and cell wall integrity (Qin et al., 2022; Zhang et al., 2019). Specifically, chitin helps maintain the ability of cells to grow and resist environmental stressors. Deletion of *CHS5* and *CHS7* in the ascomycete *Fusarium verticillioides* showed that the presence of CFW in the medium caused increased inhibition in both deletion strains whereas hydrogen peroxide did not affect the *CHS7* deletion strain (Larson et al., 2011). Given that chitin usually binds and anchors β -glucan to the cell membrane; increased impacts on stressors targeting chitin, β -glucan, and the cell membrane are expected as a missing *chs* gene coupled with these inhibitors should exacerbate the impacts of the stressor. When investigated in *P. ostreatus*, Δ *chs2–4* strains were significantly more sensitive to CFW, a chitin inhibitor; MCF, a β -glucan synthesis inhibitor; and SDS, a membrane stressor (Fig. 7). All strains showed a slightly increased though non-significant sensitivity to hydrogen peroxide, indicating that *chs* in *P. ostreatus* are likely specific to functions surrounding the cell wall and membrane and does not play a large role in overall cell oxidation or respiration. When grown in the presence of inhibitors all strains exhibited unstable growth in addition to sensitivity changes growing in a distorted circular manner causing instability and variation within diameter measurements. Significantly thinner cell walls and changed binding capacity to CFW also likely play an important role in increasing sensitivity and instability to cell wall-perturbing agents. Furthermore, abnormal mycelium formation probably decreases overall mycelial integrity and adds to decreased stress resistance.

Functional analysis of *chs2–4* genes also highlighted differences

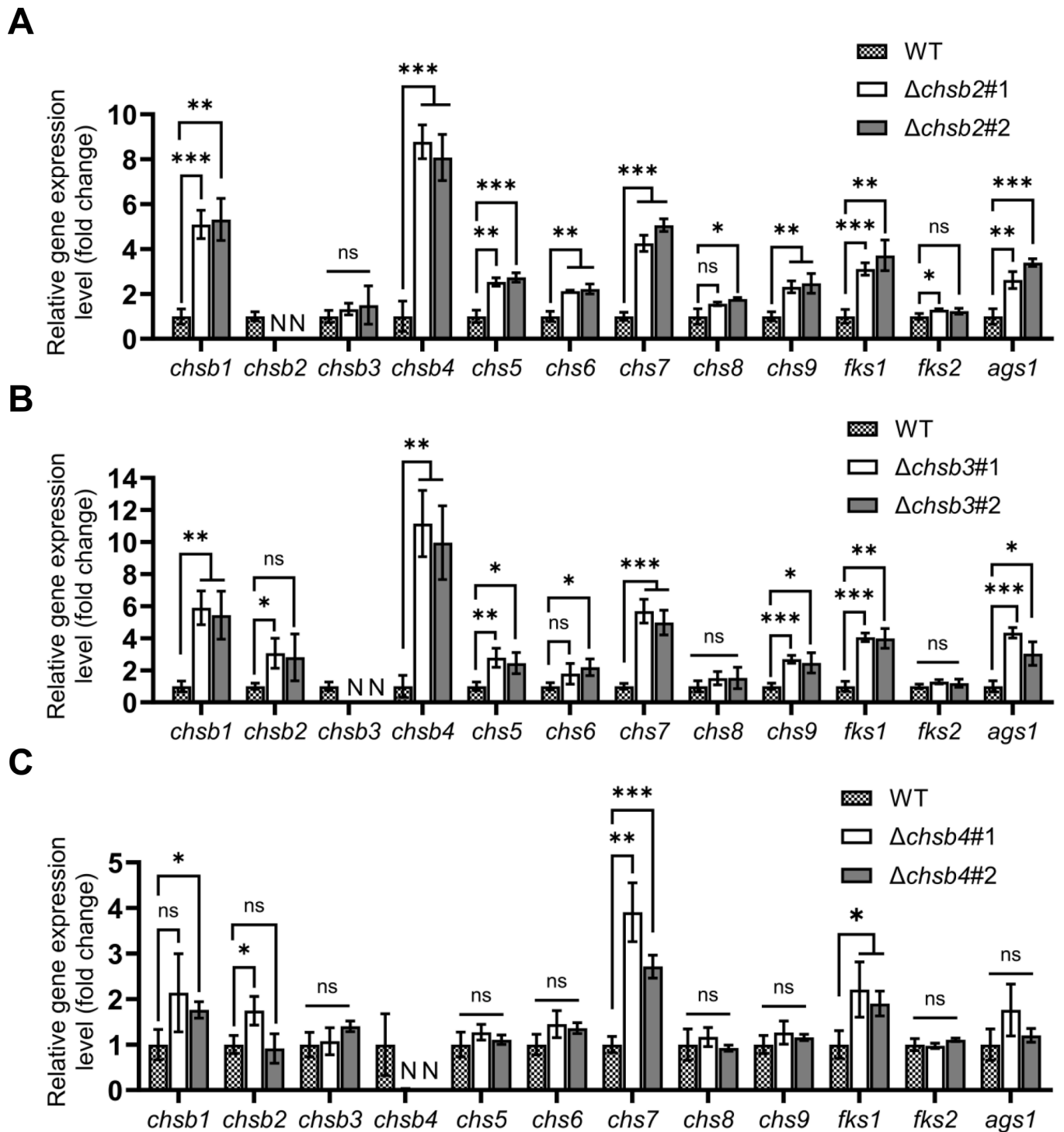
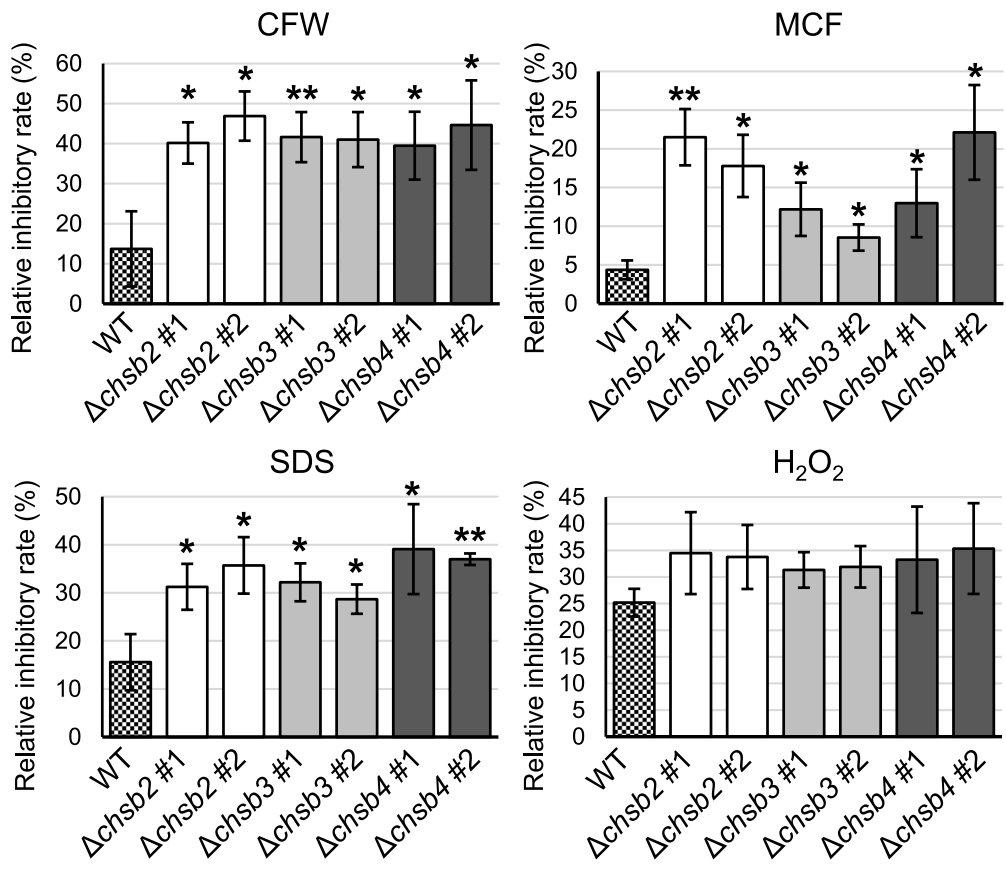
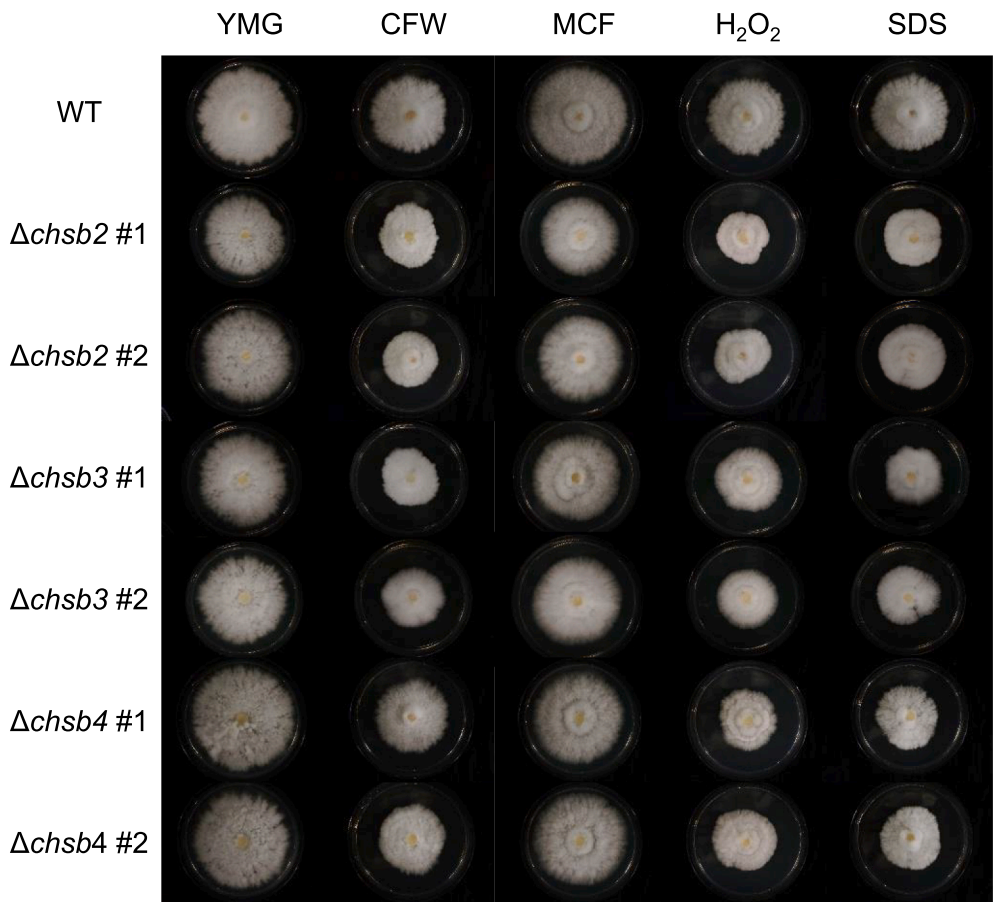


Fig. 6. Relative gene expression levels of various cell wall synthases in (A) Δ chs2, (B) Δ chs3, and (C) Δ chs4 strains. The bars indicate the standard deviations of three biological replicates ($n = 3$). Statistical significance was determined using a two-tailed equal variance t -test ($*P < 0.05$, $**P < 0.01$, $***P < 0.001$, WT; wild-type N; Gene expression not detected, ns; not significant).

between ascomycete and basidiomycete *chs* genes, as *chs2–4* often behave differently from known functions of various ascomycete *chs* genes. In the ascomycetes *Monascus purpureus* and *Metarhizium acridum*, deletion of CHSs led to a large increase in chitin content (Shu et al., 2022; Zhang et al., 2019); however, this was not observed in *P. ostreatus*. Furthermore, multiple studies in ascomycetes have suggested that this increase in chitin content after *chs* gene disruption (20–50 % higher) was due to the overexpression of various other chitin synthases as an overcompensation for the lost gene (Cui et al., 2013; Larson et al., 2011; Shu

et al., 2022). Our results, on the other hand, indicate that despite the high overexpression of many other *chs* genes relative percentage of chitin does not increase; rather, *chs*b disruption seems to decrease the amount of chitin available per length of mycelium and cause thinner cell walls and mycelium defects. Therefore, CHSs in basidiomycetes have different roles and functions than those in ascomycetes. Additionally, filamentous ascomycetes often have higher levels of chitin (up to 40 % of the dry weight) (Rogg et al., 2012); whereas *P. ostreatus* chitin is much lower at around 4 %, despite having a similar number of chitin synthase



(caption on next page)

Fig. 7. Stress response of mycelia in the wild-type (WT) and *chs*b disruptants. (A) Phenotypes of all strains grown on yeast and malt extract with glucose (YMG) agar medium supplemented with 5 mM H₂O₂, 0.02 % sodium dodecyl sulphate (SDS), 100 µg/ml micafungin (MCF), and 500 µg/ml calcofluor-white (CFW) for 10 days. (B) The relative growth inhibition rates of all the strains in (A). Bars indicate standard deviations of three biological replicates (*n* = 3). Statistical significance was determined using a two-tailed equal variance *t*-test (**P* < 0.05, ***P* < 0.01).

genes. Therefore, gene regulation and chitin synthesis are different between phyla. In this study, we demonstrated the essential role of *chs*b genes in the formation of vegetative mycelia. Given their basidiomycete-specific phylogeny, it would also be interesting to determine whether these genes have a special function in sexual development. A previous gene expression study suggested that agaricomycetes CHSs may have unique functions in fruiting body formation, as *chs*b3 has been reported to be highly expressed in *P. ostreatus* primordia and is upregulated by more than fourfold relative to vegetative mycelia. Suggesting that although *chs*b2 and *chs*b3 are in the same clade they may have slightly different functions and are not fully redundant with each other. Furthermore, the expression of *chs*b3 in the primordia is conserved among 12 agaricomycete species (Nagy et al., 2023). Further studies on *chs*b function during sexual development are ongoing.

5. Conclusion

This study highlights the important roles of basidiomycete chitin synthases and provides insights into the evolution and function of agaricomycete *chs* genes. The results identified three clades of basidiomycete-specific *chs* genes and for the first time, the physiological functions of white-rot and agaricomycete CHSs. In *P. ostreatus*, the basidiomycete-specific genes *chs*b2–4 play important roles in normal cell wall, mycelial, and aerial hyphae formation. Disruption of *chs*b2–4 caused significantly decreased cell wall thickness, shorter aerial hyphae, and differential expression of various cell wall synthases; however, did not alter relative amounts of chitin and β-glucan. This suggests that disruption of these genes decreases the amount of chitin available per unit length of mycelia. The results also highlighted that *chs*b2 and *chs*b3 disrupted strains were functionally similar to each other, whereas *chs*b4 disrupted strains were slightly different, which corresponds to the phylogenetic classification. Understanding the phylogeny and function of these genes is critical for improving our understanding of basidiomycete cell wall synthesis and for providing novel insights into agaricomycete CHS functions, basidiomycete evolution in filamentous fungi, and basidiomycete-specific cell wall roles.

CRedit authorship contribution statement

Kim Schiphof: Writing – original draft, Visualization, Methodology, Investigation, Formal analysis, Data curation, Conceptualization. **Moriyuki Kawachi:** Writing – review & editing, Visualization, Supervision, Resources, Methodology, Funding acquisition, Formal analysis, Conceptualization. **Kenya Tsuji:** Resources, Funding acquisition, Data curation. **Akira Yoshimi:** Resources, Funding acquisition, Data curation. **Chihiro Tanaka:** Resources, Project administration, Data curation. **Takehito Nakazawa:** Methodology, Data curation. **Yoichi Honda:** Writing – review & editing, Resources, Project administration, Data curation, Conceptualization.

Declaration of competing interest

The authors declare that they have no known competing financial interests or personal relationships that could have appeared to influence the work reported in this paper.

Data availability

Data will be made available on request.

Acknowledgments

The authors thank Prof. Yitzhak Hadar (Hebrew University of Jerusalem) for providing *P. ostreatus* strain 20b. We thank the Division of Electron Microscopic Study, Centre for Anatomical Studies, Graduate School of Medicine, Kyoto University for technical assistance with electron microscopy.

Funding

This work was supported in part by the Institute for Fermentation, Osaka, Japan [K-2019-002 to M. K. and K. T.], Grants-in-Aid for Scientific Research from the Japan Society for the Promotion of Science [22H02238 to A. Y. and M. K., 22K05763 to M. K.], and JSPS Bilateral Program [JPJSBP 120238807 to M. K.].

Appendix A. Supplementary data

Supplementary data to this article can be found online at <https://doi.org/10.1016/j.fgb.2024.103893>.

References

- Abo Elsaid, M.M., El Kady, E.M., 2019. Current trends in fungal biosynthesis of chitin and chitosan. *Bull. Natl. Res. Cent.* 43, 59. <https://doi.org/10.1186/s42269-019-0105-y>.
- Altschul, S.F., Gish, W., Miller, W., Myers, E.W., Lipman, D.J., 1990. Basic local alignment search tool. *J. Mol. Biol.* 215, 403–410. [https://doi.org/10.1016/s0022-2836\(05\)80360-2](https://doi.org/10.1016/s0022-2836(05)80360-2).
- Banks, I.R., Specht, C.A., Donlin, M.J., Gerik, K.J., Levitz, S.M., Lodge, J.K., 2005. A chitin synthase and its regulator protein are critical for chitosan production and growth of the fungal pathogen *Cryptococcus neoformans*. *Eukaryot. Cell.* 4, 1902–1912. <https://doi.org/10.1128/ec.4.11.1902-1912.2005>.
- Basenko, E.Y., Pulman, J.A., Shanmugasundram, A., Harb, O.S., Crouch, K., Starns, D., Warrenfeltz, S., Aurecochea, C., Stoeckert Jr, C.J., Kissinger, J.C., Roos, D.S., Hertz-Fowler, C., 2018. FungiDB: an integrated bioinformatic resource for fungi and oomycetes. *J. Fungi.* 4, 39. <https://doi.org/10.3390/jof4010039>.
- Boureghda, Y., Satha, H., Bendebane, F., 2021. Chitin-glucan complex from pleurotus ostreatus mushroom: physicochemical characterization and comparison of extraction methods. *Waste Biomass Valor.* 12, 6139–6153. <https://doi.org/10.1007/s12649-021-01449-3>.
- Broeker, K., Fehser, S., Moerschbacher, B.M., 2006. Survey and expression analysis of five new chitin synthase genes in the biotrophic rust fungus *Puccinia graminis*. *Curr. Genet.* 50, 295–305. <https://doi.org/10.1007/s00294-006-0094-x>.
- Brown, C., Patrick, J., Liebau, J., Mäler, L., 2022. The MIT domain of chitin synthase 1 from the oomycete *Saprolegnia monoica* interacts specifically with phosphatidic acid. *Biochem. Biophys. Res. Commun.* 30, 101229. <https://doi.org/10.1016/j.bbrep.2022.101229>.
- Chen, D.-D., Wang, Z.-B., Wang, L.-X., Zhao, P., Yun, C.-H., Bai, L., 2023. Structure, catalysis, chitin transport, and selective inhibition of chitin synthase. *Nat. Commun.* 14, 4776. <https://doi.org/10.1038/s41467-023-40479-4>.
- Choi, H., Kim, S.L., Jeong, M.-K., Yu, O.H., Eyun, S., 2022. Identification and phylogenetic analysis of chitin synthase genes from the deep-sea polychaete *Branchiopolyno onnuriensis* genome. *J. Mar. Sci. Eng.* 10, 598. <https://doi.org/10.3390/jmse10050598>.
- Cui, Z., Wang, Y., Lei, N., Wang, K., Zhu, T., 2013. *Botrytis cinerea* chitin synthase BcChsVI is required for normal growth and pathogenicity. *Curr. Genet.* 59, 119–128. <https://doi.org/10.1007/s00294-013-0393-y>.
- Cummings, W.J., Celerin, M., Crodian, J., Brunick, L.K., Zolan, M.E., 1999. Insertional mutagenesis in *Coprinus cinereus*: use of a dominant selectable marker to generate tagged, sporulation-defective mutants. *Curr. Genet.* 36, 371–382. <https://doi.org/10.1007/s002940050512>.
- Dalonso, N., Petkowicz, C.L.O., Lugones, L.G., Silveira, M.L.L., Gern, R.M.M., 2021. Comparison of cell wall polysaccharides in *Schizophyllum commune* after changing phenotype by mutation. *An. Acad. Bras. Cienc.* 93, e20210047. <https://doi.org/10.1590/0001-3765202120210047>.
- Ehren, H.L., Appels, F.V.W., Houben, K., Renault, M.A.M., Wösten, H.A.B., Baldus, M., 2020. Characterization of the cell wall of a mushroom forming fungus at atomic resolution using solid-state NMR spectroscopy. *Cell Surf.* 6, 100046. <https://doi.org/10.1016/j.tcs.2020.100046>.
- Ene, I.V., Walker, L.A., Schiavone, M., Lee, K.K., Martin-Yken, H., Dague, E., Gow, N.A., Munro, C.A., Brown, A.J., 2015. Cell wall remodeling enzymes modulate fungal cell

- wall elasticity and osmotic stress resistance. *mBio* 6, e00986. <https://doi.org/10.1128/mBio.00986-15>.
- Fernando, L.D., Dickwella Widanage, M.C., Penfield, J., Lipton, A.S., Washton, N., Latgé, J.-P., Wang, P., Zhang, L., Wang, T., 2021. Structural polymorphism of chitin and chitosan in fungal cell walls from solid-state NMR and principal component analysis. *Front. Mol. Biosci.* 8, 727053 <https://doi.org/10.3389/fmolb.2021.727053>.
- Gonçalves, I.R., Brouillet, S., Soulié, M.-C., Gribaldo, S., Sirven, C., Charron, N., Boccara, M., Choquer, M., 2016. Genome-wide analyses of chitin synthases identify horizontal gene transfers towards bacteria and allow a robust and unifying classification into fungi. *BMC Evol. Biol.* 16, 252. <https://doi.org/10.1186/s12862-016-0815-9>.
- Gong, Z., Zhang, S., Liu, J., 2023. Recent advances in chitin biosynthesis associated with the morphology and secondary metabolite synthesis of filamentous fungi in submerged fermentation. *J. Fungi*. 9, 205. <https://doi.org/10.3390/jof9020205>.
- Gow, N.A.R., Latge, J.-P., Munro, C.A., 2017. The fungal cell wall: structure, biosynthesis, and function. *Microbiol. Spectr.* 5 <https://doi.org/10.1128/microbiolspec.FUNK-0035-2016>.
- Hallgren, J., Hallgren, J., Tsigos, K.D., Pedersen, M.D., Almagro Armenteros, J.J., Marcatili, P., Nielsen, H., Krogh, A., Winther, O., 2022. DeepTMHMM predicts alpha and beta transmembrane proteins using deep neural networks. *BioRxiv* 2022. <https://doi.org/10.1101/2022.04.08.487609>.
- Han, J., Kawauchi, M., Schiphof, K., Terauchi, Y., Yoshimi, A., Tanaka, C., Nakazawa, T., Honda, Y., 2023. Features of disruption mutants of genes encoding for hydrophobin Vmh2 and Vmh3 in mycelial formation and resistance to environmental stress in *Pleurotus ostreatus*. *FEMS Microbiol. Lett.* 370, fnad036 <https://doi.org/10.1093/femsle/fnad036>.
- Haneef, M., Ceseracciu, L., Canale, C., Bayer, I.S., Heredia-Guerrero, J.A., Athanassiou, A., 2017. Advanced materials from fungal mycelium: fabrication and tuning of physical properties. *Sci. Rep.* 7, 41292. <https://doi.org/10.1038/srep41292>.
- Hole, C.R., Lam, W.C., Upadhyay, R., Lodge, J.K., 2020. *Cryptococcus* neoformans chitin synthase 3 plays a critical role in dampening host inflammatory responses. *mBio* 11, e03373-e10419. <https://doi.org/10.1128/mBio.03373-19>.
- Ichinomiya, M., Yamada, E., Yamashita, S., Ohta, A., Horiuchi, H., 2005. Class I and class II chitin synthases are involved in septum formation in the filamentous fungus *Aspergillus nidulans*. *Eukaryot. Cell.* 4, 1125–1136. <https://doi.org/10.1128/ec.4.6.1125-1136.2005>.
- Izumitsu, K., Hatoh, K., Sumita, T., Kitade, Y., Morita, A., Gafur, A., Ohta, A., Kawai, M., Yamanaka, T., Neda, H., Ota, Y., Tanaka, C., 2012. Rapid and simple preparation of mushroom DNA directly from colonies and fruiting bodies for PCR. *Mycoscience*. 53, 396–401. <https://doi.org/10.1007/S10267-012-0182-3>.
- Jin, J., Iwama, R., Takagi, K., Horiuchi, H., 2021. AP-2 complex contributes to hyphal-tip-localization of a chitin synthase in the filamentous fungus *Aspergillus nidulans*. *Fungal Biol.* 125, 806–814. <https://doi.org/10.1016/j.funbio.2021.05.009>.
- Jones, P., Binns, D., Chang, H.Y., Fraser, M., Li, W., McAnulla, C., McWilliam, H., Maslen, J., Mitchell, A., Nuka, G., Pesseat, S., Quinn, A.F., Sangrador-Vegas, A., Scheremetjew, M., Yong, S.Y., Lopez, R., Hunter, S., 2014. InterProScan 5: genome-scale protein function classification. *Bioinformatics*. 30, 1236–1240. <https://doi.org/10.1093/bioinformatics/btu031>.
- Larson, T.M., Kendra, D.F., Busman, M., Brown, D.W., 2011. *Fusarium verticillioides* chitin synthases *CHS5* and *CHS7* are required for normal growth and pathogenicity. *Curr. Genet.* 57, 177–189. <https://doi.org/10.1007/s00294-011-0334-6>.
- Li, M., Jiang, C., Wang, Q., Zhao, Z., Jin, Q., Xu, J.-R., Liu, H., 2016. Evolution and functional insights of different ancestral orthologous clades of chitin synthase genes in the fungal tree of life. *Front. Plant Sci.* 7, 37. <https://doi.org/10.3389/fpls.2016.00037>.
- Liu, R., Xu, C., Zhang, Q., Wang, S., Fang, W., 2017. Evolution of the chitin synthase gene family correlates with fungal morphogenesis and adaptation to ecological niches. *Sci. Rep.* 7, 44527. <https://doi.org/10.1038/srep44527>.
- Muraguchi, H., Ito, Y., Kamada, T., Yanagi, S.O., 2003. A linkage map of the basidiomycete *Coprinus cinereus* based on random amplified polymorphic DNAs and restriction fragment length polymorphisms. *Fungal Genet. Biol.* 40, 93–102. [https://doi.org/10.1016/S1087-1845\(03\)00087-2](https://doi.org/10.1016/S1087-1845(03)00087-2).
- Nagy, L.G., Vonk, P.J., Künzler, M., Földi, C., Virágh, M., Ohm, R.A., Hennicke, F., Bálint, B., Csernetics, Á., Hegedüs, B., Hou, Z., Liu, X.B., Nan, S., Pareek, M., Sahu, N., Szathmári, B., Varga, T., Wu, H., Yang, X., Merényi, Z., 2023. Lessons on fruiting body morphogenesis from genomes and transcriptomes of Agaricomycetes. *Stud. Mycol.* 104, 1–85. <https://doi.org/10.3114/sim.2022.104.01>.
- Nakazawa, T., Tsuzuki, M., Irie, T., Sakamoto, M., Honda, Y., 2016. Marker recycling via 5-fluoroorotic acid and 5-fluorocytosine counter-selection in the white-rot agaricomycete *Pleurotus ostreatus*. *Fungal Biol.* 120, 1146–1155. <https://doi.org/10.1016/j.funbio.2016.06.011>.
- Nishihara, M., Watanabe, A., Asada, Y., 2007a. Isolation and characterization of the gene encoding a chitin synthase with a myosin motor-like domain from the edible basidiomycetous mushroom, *Lentinula edodes*, and its expression in the course of fruit-body formation. *Mycoscience* 48, 109–116. <https://doi.org/10.1007/S10267-006-0339-Z>.
- Nishihara, M., Watanabe, A., Asada, Y., 2007b. Isolation, characterization, and expression analysis of a class IV chitin synthase gene from the edible basidiomycetous mushroom *Pleurotus ostreatus*. *Mycoscience* 48, 176–181. <https://doi.org/10.1007/s10267-006-0342-4>.
- Nordberg, H., Cantor, M., Dusheyko, S., Hua, S., Poliakov, A., Shabalov, I., Smirnova, T., Grigoriev, I.V., Dubchak, L., 2014. The genome portal of the Department of Energy Joint Genome Institute: 2014 updates. *Nucleic Acids Res.* 42, D26–D31. <https://doi.org/10.1093/nar/gkt1069>.
- Pacheco-Arjona, J.R., Ramirez-Prado, J.H., 2014. Large-scale phylogenetic classification of fungal chitin synthases and identification of a putative cell-wall metabolism gene cluster in *Aspergillus* genomes. *PLoS One* 9, e104920.
- Pfaffl, M.W., 2001. A new mathematical model for relative quantification in real-time RT-PCR. *Nucleic Acids Res.* 29, e45.
- Qin, J., Zhao, P., Ye, Z., Sun, L., Hu, X., Zhang, J., 2022. Chitin synthase genes are differentially required for growth, stress response, and virulence in *Verticillium dahliae*. *J. Fungi*. 8, 681. <https://doi.org/10.3390/jof8070681>.
- Rao, P.S., Niederpruem, D.J., 1969. Carbohydrate metabolism during morphogenesis of *Coprinus lagopus* (sensu Buller). *J. Bacteriol.* 100, 1222–1228. <https://doi.org/10.1128/jb.100.3.1222-1228.1969>.
- Rogg, L.E., Fortwendel, J.R., Juvvadi, P.R., Steinbach, W.J., 2012. Regulation of expression, activity and localization of fungal chitin synthases. *Med. Mycol.* 50, 2–17. <https://doi.org/10.3109/13693786.2011.577104>.
- Salame, T.M., Knop, D., Tal, D., Levinson, D., Yarden, O., Hadar, Y., 2012. Predominance of a versatile-peroxidase-encoding gene, *mmp4*, as demonstrated by gene replacement via a gene targeting system for *Pleurotus ostreatus*. *Appl. Environ. Microbiol.* 78, 5341–5352. <https://doi.org/10.1128/aem.01234-12>.
- Sato, T., Okawa, K., Hirano, T., 2010. Cloning and characterization of a *Lentinula edodes* Class II chitin synthase gene, *LeChs2*. *Biosci. Biotech. Biochem.* 74, 1707–1709. <https://doi.org/10.1271/bbb.100222>.
- Shu, M., Lu, P., Liu, S., Zhang, S., Gong, Z., Cai, X., Zhou, B., Lin, Q., Liu, J., 2022. Disruption of the chitin biosynthetic pathway results in significant changes in the cell growth phenotypes and biosynthesis of secondary metabolites of *Monascus purpureus*. *J. Fungi*. 8, 910. <https://doi.org/10.3390/jof8090910>.
- Silverman, S.J., Sbrulati, A., Slater, M.L., Cabib, E., 1988. Chitin synthase 2 is essential for septum formation and cell division in *Saccharomyces cerevisiae*. *Proc. Natl. Acad. Sci. U.S.A.* 85, 4735–4739. <https://doi.org/10.1073/pnas.85.13.4735>.
- Soria, N.W., Díaz, M.S., Figueroa, A.C., Alasino, V.R., Yang, P., Beltramo, D.M., 2021. Identification of Chitin synthase and Chitinase genes in three ontogenetic stages from *Thecaphora frezii*, the causal agent of peanut smut disease. *Phys. Mol. Plant Pathol.* 116, 101727 <https://doi.org/10.1016/j.pmp.2021.101727>.
- Sreenivasaprasad, S., Burton, K.S., Wood, D.A., 2000. Cloning and characterisation of a chitin synthase gene cDNA from the cultivated mushroom *Agaricus bisporus* and its expression during morphogenesis. *FEMS Microbiol. Lett.* 189, 73–77. <https://doi.org/10.1111/j.1574-6968.2000.tb09208.x>.
- Tamura, K., Stecher, G., Kumar, S., 2021. MEGA11: molecular evolutionary genetics analysis version 11. *Mol. Biol. Evol.* 38, 3022–3027. <https://doi.org/10.1093/molbev/msab120>.
- Wang, S., Shi, L., Hu, Y., Liu, R., Ren, A., Zhu, J., Zhao, M., 2018. Roles of the *Skn7* response regulator in stress resistance, cell wall integrity and GA biosynthesis in *Ganoderma lucidum*. *Fungal Genet. Biol.* 114, 12–23. <https://doi.org/10.1016/j.fgb.2018.03.002>.
- Zhang, J., Jiang, H., Du, Y., Keyhani, N.O., Xia, Y., Jin, K., 2019. Members of chitin synthase family in *Metarhizium acridum* differentially affect fungal growth, stress tolerances, cell wall integrity and virulence. *PLoS Pathog.* 15, e1007964.
- Zhou, J., Kang, L., Liu, C., Niu, X., Wang, X., Liu, H., Zhang, W., Liu, Z., Latgé, J.-P., Yuan, S., 2019. Chitinases play a key role in stipe cell wall extension in the mushroom *Coprinopsis cinerea*. *Appl. Environ. Microbiol.* 85, e00532–e619. <https://doi.org/10.1128/AEM.00532-19>.
- Zolan, M.E., Pukkila, P.J., 1986. Inheritance of DNA methylation in *Coprinus cinereus*. *Mol. Cell Biol.* 6, 195–200. <https://doi.org/10.1128/mcb.6.1.195-200.1986>.